Research Article

Zuhur Alqahtani, Ibrahim Abbas*, Alaa A. El-Bary, and Areej Almuneef

Nonlinear analysis of generalized thermoelastic interaction in unbounded thermoelastic media

https://doi.org/10.1515/cls-2024-0024 received September 02, 2024; accepted April 16, 2025

Abstract: The transient response of thermoelastic materials subjected to a time-decaying thermal field is presented in this article using a nonlinear analysis. The basic equations provided are based on a generalized thermoelastic model under changing thermal conductivity, which is incorporated into the formulations. This problem is solved using the finite-element techniques instead of the Kirchhoff transforms since solving non-linear equations is quite difficult. Laplace transformation and the eigenvalue approaches are used to solve the problems in the linear context of the Kirchhoff transforms. The study investigates and compares the impact of varying thermal conductivity both with and without employing Kirchhoff's transform. The numerical outputs are graphically shown to display the displacement, temperature, and stress variations.

Keywords: Kirchhoff's transforms, variable thermal conductivity, Laplace transforms, eigenvalues approaches, finite-element method

Nomenclature

 $egin{array}{ll} u_i & ext{Displacement components} \ \omega & ext{Decayed heat flux exponent} \ T & ext{Medium temperature} \ K_1 & ext{Non-positive parameter} \ \end{array}$

Zuhur Alqahtani: Department of Mathematical Sciences, College of Science, Princess Nourah bint Abdulrahman University, P.O. Box 84428, Riyadh, 11671, Saudi Arabia, e-mail: zumalqahtani@pnu.edu.sa

Alaa A. El-Bary: Institute of Basic and Applied Science, Arab Academy for Science, Technology and Maritime Transport, Alexandria, Egypt, e-mail: aaelbary@aast.edu

Areej Almuneef: Department of Mathematical Sciences, College of Science, Princess Nourah bint Abdulrahman University, P.O. Box 84428, Riyadh, 11671, Saudi Arabia, e-mail: aaalmuneef@pnu.edu.sa

 τ_o Thermal relaxation time Components of the stress σ_{ii} Kronecker symbol δ_{ij} Thermal conductivity when $T = T_0$ K_o Specific heat c_e λ, μ Lame's constants T_o Initial temperature of the medium Linear thermal expansion coefficient α_t Mass density of tissue ρ Strain components k Tissue thermal conductivity time

1 Introduction

Earlier perspectives presumed the independence of all thermal parameters in thermoelasticity models from temperature fluctuations. However, a more nuanced understanding emerged as Noda [1] extensively analyzed materials in 1991, demonstrating that thermal conductivity exponentially decreases with increasing temperature. The importance of thermoelastic material with varying thermal conductivity has increased, finding recent applications in intriguing fields, particularly in cutting-edge technology, notably within emerging energy sources.

In the thermoelastic field, employing the classical elastic model for heating conduction is well-suited for a wide range of engineering applications. Nevertheless, in scenarios involving ultrafast heating, the classical model falls short in providing precise temperature approximations. Generalized thermoelastic theory, which characterizes the interaction between mechanical and thermal loads in materials, introduces thermoelastic disturbances that propagate as waves with speeds more closely reflecting real-world behavior compared to the classical model proposed by Biot [2]. Consequently, to address these limitations and enhance the accuracy of temperature distribution determinations, various non-classical thermoelastic theories, including the Lord and Shulman (LS) [3] and Green and Naghdi [4,5] models, have been introduced.

As temperatures rise, it is conceivable that the properties of the materials may experience a reduction.

^{*} Corresponding author: Ibrahim Abbas, Mathematics Department, Faculty of Science, Sohag University, Sohag, Egypt, e-mail: ibrabbas7@science.sohag.edu.eg

2 — Zuhur Algahtani et al. DE GRUYTER

In numerous materials, the thermal conductivity (*K*) typically reduces nearly linearly with rising absolute temperature (*T*) [6]. To solve the problem associated with varying thermal conductivity [7], Kirchhoff's transformation mapping technique [6] is applied. For a one-dimensional problem involving varying material parameters, Mukhopadhyay and Kumar [8] employed the finite differences method.

Sherief and Hamza [9] proposed a model to account for the change in thermal conductivity in thermoelastic cylinders extending to infinity. Abbas et al. [10] investigated the interactions between light and heat within a semiconductor material featuring a cylindrical hole and changed thermal conductivity. Othman et al. [11] investigated the impacts of initial stress and varying thermal conductivity in infinite fibre-reinforced plates. Ghasemi et al. [12] studied the thermal analysis studying on convective fins with changes in thermal conductivity and heating generation. Xiong et al. [13] discussed analyzing the impacts of change thermal conduction in thermoelastic interactions within an anisotropic fiber-reinforced medium. Khoukhi et al. [14] examined the influence of changing thermal conductivity on transient temperature fluctuation within wallembedded insulations. Abbas [15] utilized a finite-element approach to study magneto-thermoelasticity interactions in inhomogeneous isotropic cylinders. Xiong and Guo [16] investigated the impact of movable heat sources and varying properties in the context of magneto-thermoelastic, employing a fractional thermoelasticity theory. Zenkour and Abbas [17] examined a scenario that included density and thermoelastic properties varying with temperature, revealing important characteristics of materials exhibiting such temperature-dependent properties. Othman [18] investigated thermoelastic interaction in a two-dimensional thermoelasticity problem with temperature-dependence elastic modulus. Aboueregal and Sedighi [19] applied the Moore-Gibson-Thompson theory to examine the influences of rotations and evolving properties in visco-thermoelasticity anisotropic cylinders. The model considers the impacts of rotations and evolving properties, which can have a significant effect on heat transfer. Youssef and Abbas [20] conducted research on an unbounded medium containing spherical cavities, exploring how the heat conductive and elastic modulus change with temperature in materials. Several experimental and theoretical inquiries have consistently demonstrated a substantial association between temperature variations and thermal conductivity. Proposed solutions for a variety of issues have been derived through the utilization of extended thermoelastic models [21-40].

In this work, the effects of changes in relaxation time and thermal conductivity on the propagation of thermoelastic waves in different materials are going to be investigated. The nonlinear problems were solved by the finite-element methods (FEMs) without the necessity for the Kirchhoff transformation. Using eigenvalue analysis and Laplace transforms, solutions were found for the linear problems that included Kirchhoff's transformations. The numerical results for various physical parameters were acquired and shown graphically. Through a close examination of the solution's behavior, this study sought to confirm the accuracy and reliability of the proposed approach.

2 Basic equations

Consider elastic materials with constant elastic parameters, adhering to the fundamental relations within the framework of the generalized thermoelastic model. This model, which involves one relaxation time and assumes a linear variation of thermal conductivity within a specified temperature range, is utilized. Notably, nobody forces or heat source is considered, leading to the basic formulations that can be written by [3]

$$u_{i,jj} + (\lambda + \mu)u_{j,ij} - \gamma T_{,i} = \rho \frac{\partial^2 u_i}{\partial t^2}, \quad i = 1, 2, 3, \quad (1)$$

$$(KT_{,j})_{j} = \left(1 + \tau_{o} \frac{\partial}{\partial t}\right) \left(\rho c_{e} \frac{\partial T}{\partial t} + \gamma T_{o} \frac{\partial u_{j,j}}{\partial t}\right), \quad j = 1, 2, 3, \quad (2)$$

$$\sigma_{ii} = (\lambda u_{k,k} - \gamma T)\delta_{ii} + \mu(u_{i,i} + u_{i,i}). \tag{3}$$

In this case, K refers to the thermal conductive that fluctuates with temperature and is specified as in [41]

$$K(T) = K_0(1 + K_1T).$$
 (4)

Study an elastic material whose conditions are given as a function of both time (t) and spatial variables (x). This description enables the derivation of the nonlinear Eqs. (1)–(3), as outlined in [41]

$$\rho \frac{\partial^2 u}{\partial t^2} = (2\mu + \lambda) \frac{\partial^2 u}{\partial x^2} - \gamma \frac{\partial T}{\partial x},\tag{5}$$

$$\left[1+\tau_{o}\frac{\partial}{\partial t}\right]\left(\rho c_{e}\frac{\partial T}{\partial t}+\gamma T_{o}\frac{\partial^{2} u}{\partial t\partial x}\right)=K_{o}\frac{\partial}{\partial x}\left[(1+K_{1}T)\frac{\partial T}{\partial x}\right],\tag{6}$$

$$\sigma_{xx} = (2\mu + \lambda) \frac{\partial u}{\partial x} - \gamma T.$$
 (7)

3 Application

To derive solutions for the formulations, the initial and boundary conditions can be given by

$$T(x, 0) = 0, \quad \frac{\partial T}{\partial t}\Big|_{t=0} = 0, \quad u(x, 0) = 0, \quad \frac{\partial u}{\partial t}\Big|_{t=0} = 0, \quad (8)$$

$$T(0,t) = e^{-\omega t}, \quad u(0,t) = 0.$$
 (9)

To streamline the basic equations, we can employ the following dimensionless variables:

$$(t', \tau'_o) = \eta c^2(t, \tau_o), T' = \frac{T}{T_o}, (x', u') = \eta c(x, u),$$

$$K'_1 = T_o K_1, \sigma'_{xx} = \frac{\sigma_{xx}}{\lambda + 2u},$$
(10)

where $\eta = \frac{\rho c_e}{K}$ and $c^2 = \frac{\lambda + 2\mu}{\rho}$.

In relation to the dimensionless quantities defined in Eq. (10), the basic equations above are simplified (omitting the dashed notation for convenience):

$$\frac{\partial^2 u}{\partial x^2} - a_1 \frac{\partial T}{\partial x} = \frac{\partial^2 u}{\partial t^2},\tag{11}$$

$$(1 + K_1 T) \frac{\partial^2 T}{\partial x^2} + K_1 \left[\frac{\partial T}{\partial x} \right]^2 = \left[1 + \tau_0 \frac{\partial}{\partial t} \right] \left[\frac{\partial T}{\partial t} + a_2 \frac{\partial^2 u}{\partial t \partial x} \right], \quad (12)$$

$$\sigma_{xx} = \frac{\partial u}{\partial x} - a_1 T, \tag{13}$$

$$u(0,t) = 0, T(0,t) = e^{-\omega t}.$$
 (14)

where $a_1 = \frac{\gamma T_o}{\lambda + 2\mu}$, $a_2 = \frac{\gamma}{\rho c_e}$.

3.1 Nonlinear model (FEM)

In this part, the basic equations were developed as nonlinear partial differential equations. FEMs are applied in this context to obtain solutions for Eqs. (11) and (12). The FEM, initially developed for the numerical solutions of intricate problems in structural mechanics, remains a preferred approach for complex systems. The standard processes of weak formulations, as outlined in [42,43], are utilized in these approaches. The weak non-dimensional formulation has been established through derivation from the fundamental relations. The explicit definitions of the sets of independent test functions, indicated by temperature δT and displacement δu are provided. The independent test function multiplies these controlling formulations, which are then integrated over the spatial domains in accordance with the requisite boundary conditions. Hence, the temperature and displacement nodal values can be expressed as

$$T = \sum_{n=1}^{m} N_n T_n(t), \quad u = \sum_{n=1}^{m} N_n u_n(t).$$
 (15)

Here, N points to the shape function, while m indicates how many elements there are in each node. It is important

to note that, in accordance with Galerkin's traditional methods, the shape functions and weight functions are identical. Therefore,

$$\delta u = \sum_{n=1}^{m} N_n \delta u_n, \, \delta T = \sum_{n=1}^{m} N_n \delta T_n.$$
 (16)

Subsequently, the time derivatives of the unidentified factors are computed by an implicit procedure. The weak formulations corresponding to the governing Eqs. (11) and (12) are presented below for the FEM analysis:

$$\int_{0}^{L} \frac{\partial \delta u}{\partial x} \left(\frac{\partial u}{\partial x} - a_{1}T \right) dx + \int_{0}^{L} \delta u \left(\frac{\partial^{2} u}{\partial t^{2}} \right) dx = \delta u \left(\frac{\partial u}{\partial x} - a_{1}T \right)_{0}^{L}, \quad (17)$$

$$\int_{0}^{L} \frac{\partial \delta T}{\partial x} \left[(1 + K_{1}T) \frac{\partial T}{\partial x} \right] dx + \int_{0}^{L} \delta T \left[1 + \tau_{o} \frac{\partial}{\partial t} \right] \left[\frac{\partial T}{\partial t} + a_{2} \frac{\partial^{2} u}{\partial t \partial x} \right] dx = \delta T \left[(1 + K_{1}T) \frac{\partial T}{\partial x} \right]_{0}^{L}.$$
(18)

3.2 Linear model (Kirchhoff's transform)

Now, to obtain the linearized forms of the governing equations from their original nonlinear state, Kirchhoff's transformation mapping [41] is applied to account for the variation in thermal conductivity, as defined in Eq. (4)

$$\theta = \frac{1}{K_o} \int_0^T K(T) dT.$$
 (19)

This expression defines a new function that represents heat conduction. The integration is carried out after substituting the expressions from (19) in (4), yielding the result specified in Youssef [41]

$$\theta = T + \frac{1}{2}K_1T^2,$$
 (20)

$$K_{o}\frac{\partial\theta}{\partial t} = K(T)\frac{\partial T}{\partial t}, K_{o}\frac{\partial\theta}{\partial x} = K(T)T_{,j},$$

$$K_{o}\frac{\partial^{2}\theta}{\partial x^{2}} = (K(T)T_{,j})_{,j}.$$
(21)

In linear form, the governing Eqs. (11)–(14) can be expressed as

$$\frac{\partial^2 u}{\partial x^2} - a_1 \frac{\partial \theta}{\partial x} = \frac{\partial^2 u}{\partial t^2},\tag{22}$$

$$\frac{\partial^2 \theta}{\partial x^2} = \left(1 + \tau_0 \frac{\partial}{\partial t}\right) \left(\frac{\partial \theta}{\partial t} + a_2 \frac{\partial^2 u}{\partial t \partial x}\right),\tag{23}$$

$$\sigma_{xx} = \frac{\partial u}{\partial x} - a_1 T, \tag{24}$$

$$T = \frac{1}{K_1}(-1 + \sqrt{1 + 2K_1\theta}), \tag{25}$$

$$\theta(0,t) = e^{-\omega t} + \frac{1}{2}K_1e^{-2\omega t}, \quad u(0,t) = 0.$$
 (26)

Utilizing Laplace transform on Eqs. (22)-(26),

$$\bar{f}(x,p) = L[f(x,t)] = \int_{0}^{\infty} f(x,t)e^{-pt}dt.$$
 (27)

Hence

$$\frac{\mathrm{d}^2 \bar{u}}{\mathrm{d}x^2} = p^2 \bar{u} + a_1 \frac{\mathrm{d}\bar{\theta}}{\mathrm{d}x},\tag{28}$$

$$\frac{\mathrm{d}^2 \bar{\theta}}{\mathrm{d} x^2} = p(1 + p\tau_o) \left[\bar{\theta} + a_2 \frac{\mathrm{d} \bar{u}}{\mathrm{d} x} \right],\tag{29}$$

$$\bar{\sigma}_{xx} = \frac{\mathrm{d}\bar{u}}{\mathrm{d}x} - a_1 \bar{T},\tag{30}$$

$$\bar{u}(0,t) = 0, \bar{\theta}(0,p) = \frac{1}{\omega + p} + \frac{K_1}{2(\omega + p)^2}.$$
 (31)

The vector-matrix differential equations can be rewritten using the combined equations presented in (28) and (29)

$$\frac{\mathrm{d}V}{\mathrm{d}x} = AV,\tag{32}$$

where
$$V = \begin{pmatrix} \overline{u} \\ \overline{\theta} \\ \frac{d\overline{u}}{dx} \\ \frac{d\overline{\theta}}{dx} \end{pmatrix}$$
 and $A = \begin{pmatrix} 0 & 0 & 1 & 0 \\ 0 & 0 & 0 & 1 \\ p^2 & 0 & 0 & a_1 \\ 0 & p(1+p\tau_0) & a_2p(1+p\tau_0) & 0 \end{pmatrix}$.

By employing the eigenvalue techniques, as outlined in previous works [44–52], the characteristic formulation of matrix A can be given by

$$\zeta^4 - (p^2 + (1 + \tau_o p)p + (1 + \tau_o p)pa_1a_2)\zeta^2 + p^3(1 + \tau_o p) = 0.$$
(33)

The matrix eigenvalue is characterized by the four roots of the formulation, expressed as $\pm \zeta_1$, $\pm \zeta_2$. The solutions can be provided by

$$V(x, p) = \sum_{i=1}^{2} (B_i Y_i e^{-\zeta_i x} + B_{i+1} Y_{i+1} e^{\zeta_i x}).$$
 (34)

In this equation, B_1 , B_2 , B_3 , and B_4 represent constants that are computed based on the boundary conditions of the problem. A numerical approach [53] can be employed to invert the equation and acquire the final solutions for the studying variables displacement, temperature, and stress distributions.

4 Results

Now, let us consider a numerical example to demonstrate the issue, utilizing an elastic isotropic material as the chosen material for numerical evaluations. The relevant physical data are provided as [15]

$$\lambda = 77.6 \times 10^{9} \text{ (kg)(s)}^{-2}\text{(m)}^{-1}, t = 0.5,$$

$$\mu = 38.6 \times 10^{9} \text{ (kg)(m)}^{-1}\text{(s)}^{-2}, \omega = 0.3,$$

$$T_{0} = 293 \text{ (K)}, \rho = 8.954 \times 10^{3} \text{ (kg)(m)}^{-3},$$

$$K_{0} = 3.86 \times 10^{2} \text{ (kg)(m)(s)}^{-3}\text{(K)}^{-1},$$

$$\alpha_{t} = 17.8 \times 10^{-6} \text{ (K)}^{-1}, \quad c_{s} = 3.831 \times 10^{2} \text{ (m)}^{2}\text{(s)}^{-2}\text{(K)}^{-1}.$$

We studied how temperature, displacement, and stress change over distance in a material. We used a generalized thermoelastic model that includes one thermal relaxation time for heat transfer. Numerical simulations were run to model these physical properties. The simulations considered how thermal conductivity and other factors affect the results. Some simulations included Kirchhoff transforms, and some did not. Standard values were used for the initial temperature, displacement, and stress variations. The calculations were done at a time of t = 0.5. At this point, numbers were computed to see how temperature, displacement, and stress varied with distance. Figures 1-18 show the effects of different parameter values. Some figures show the impact of thermal conductivity. Others show the differences between using and not using Kirchhoff transforms. The figures give us temperature distribution (thermal wave), displacement distribution (strain waves), and mechanical wave distributions over distance.

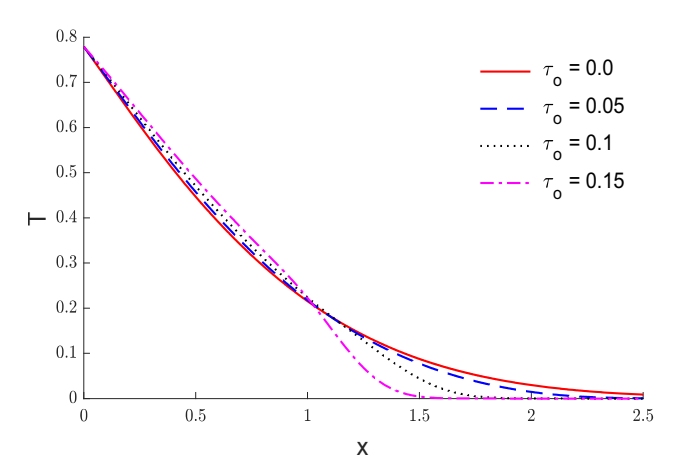


Figure 1: The effects of relaxation time in temperature variation via the distance.

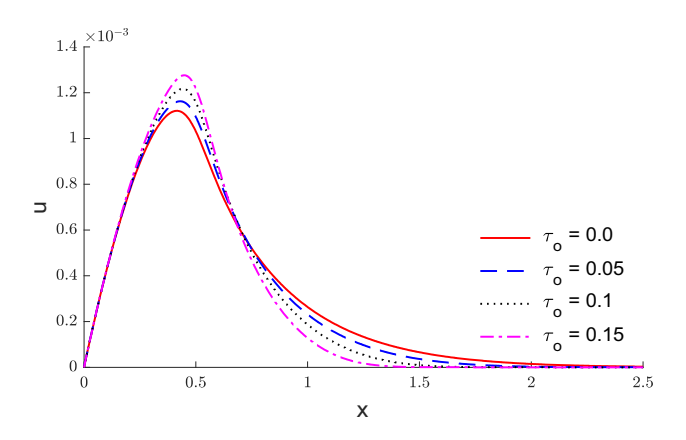


Figure 2: The effects of relaxation time in displacement variation via the distance.

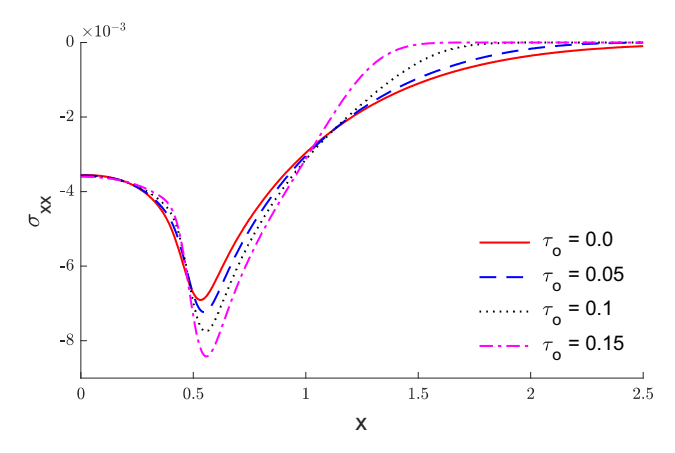


Figure 3: The impacts of relaxation time on stress variation via the distance.

Figures 1, 4, 7, 10, 13, and 16 illustrate the temperature variations across distance x. All graphs show temperature starting at maximum values $(T(0, t) = e^{\omega t})$ in accordance

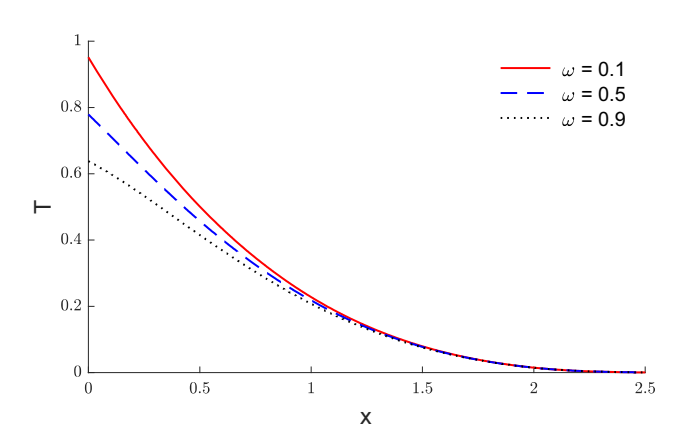


Figure 4: The effects of the exponent of decayed heating flux on the distributions of temperature via the distance.

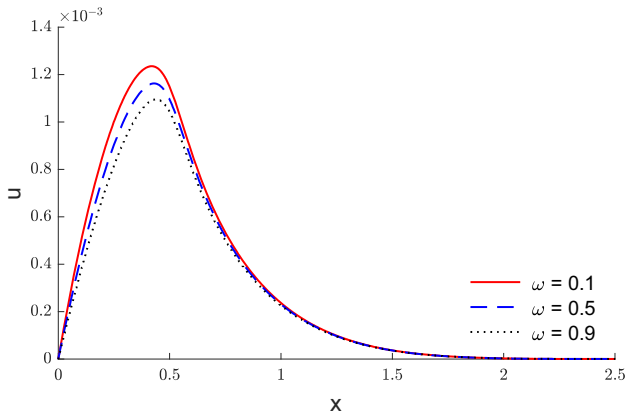


Figure 5: The effects of the exponent of decayed heating flux on the distributions of displacement via the distance.

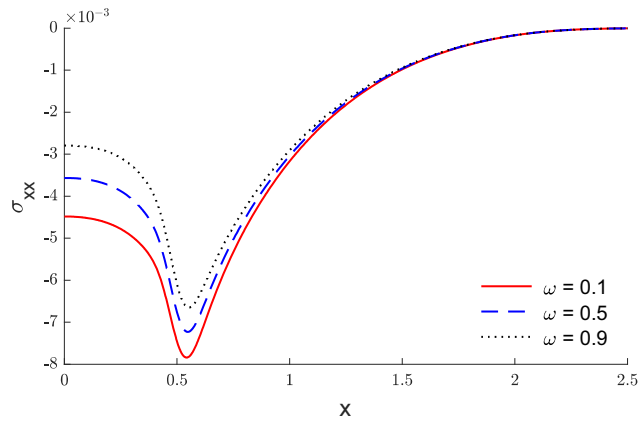


Figure 6: The effects of the exponent of decayed heating flux on the distributions of stress via the distance.

with the given boundary conditions, after which the temperature declines as x becomes larger, eventually tending toward zero. Figures 2, 5, 8, 11, 14, and 17 depict the changes

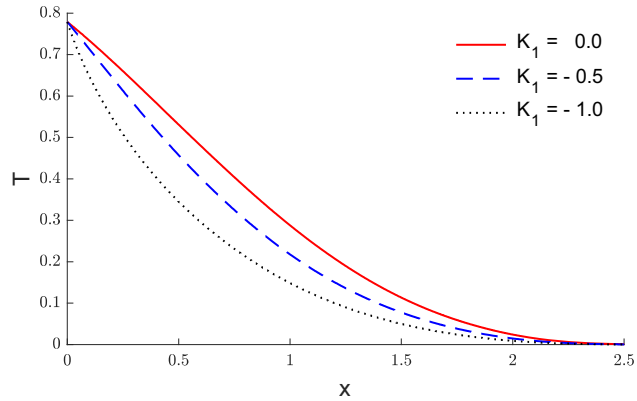


Figure 7: The temperature variations during the distances under varying thermal conductivity.

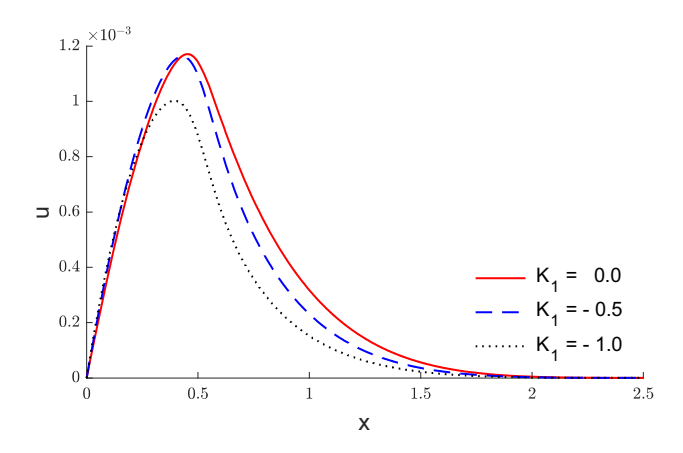


Figure 8: The displacement variation *via* the distances under varying thermal conductivity.

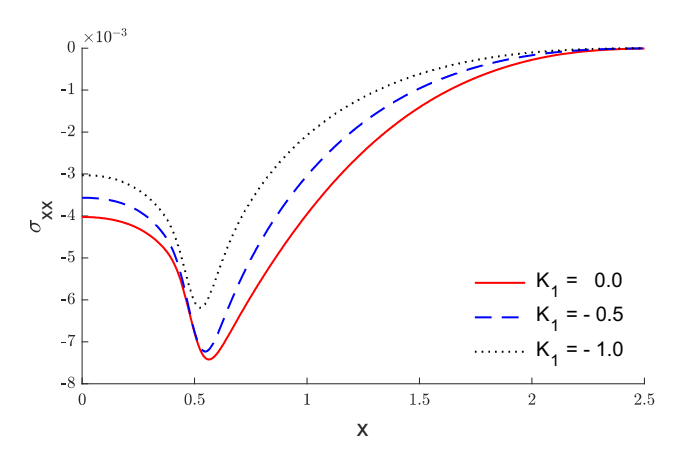


Figure 9: The stress variation *via* the distances under varying thermal conductivity.

in displacement across distance x. Notably, the displacement begins at zero in line with the given boundary conditions, after which it steadily rises to maximum levels

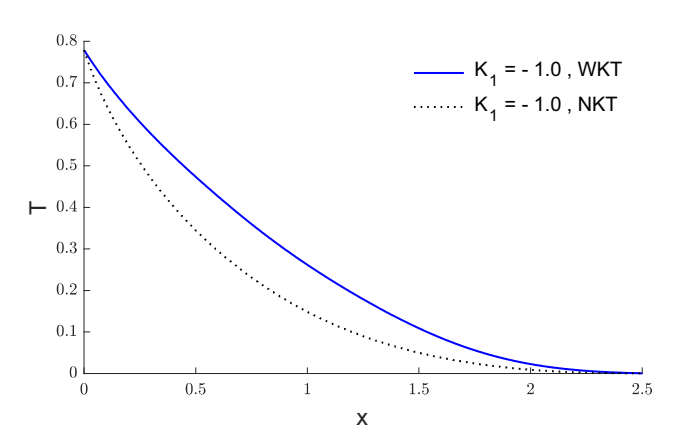


Figure 10: The temperature change at $k_1 = -1$ with and without the use of Kirchhoff's transforms.

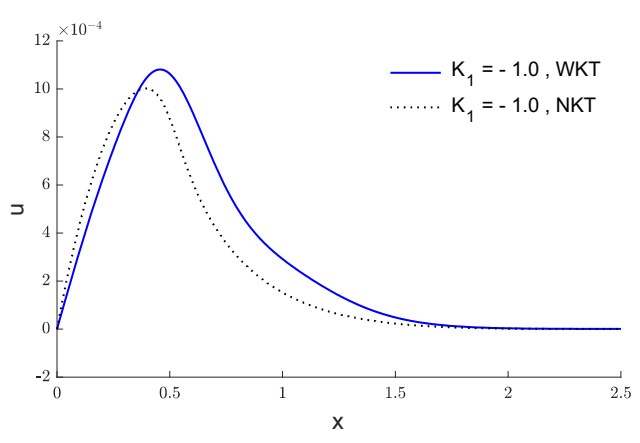


Figure 11: The displacement variations at $k_1 = -1$ with and without the use of Kirchhoff's transforms.

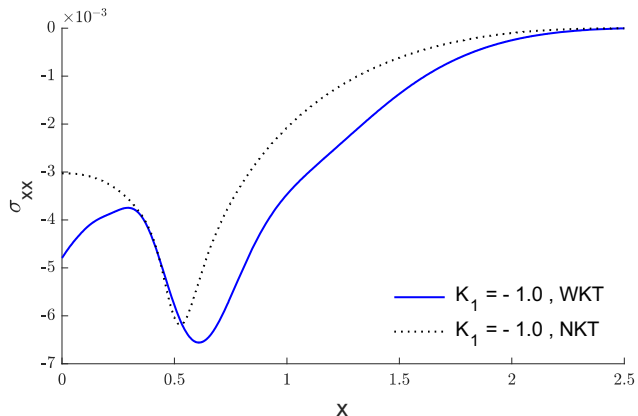


Figure 12: The stress variation at $k_1 = -1$ with and without the use of Kirchhoff's transforms.

prior to declining once more as x increases, ultimately tending towards zeros. Figures 3, 6, 9, 12, 15, and 18 depict the varying in stress via the distances x. There is evidence

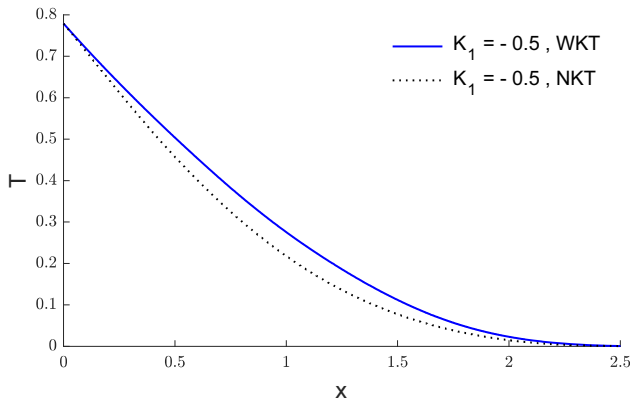


Figure 13: The temperature variation with and without the application of Kirchhoff's transform, considering the thermal conductivity parameter $k_1 = -0.5$.

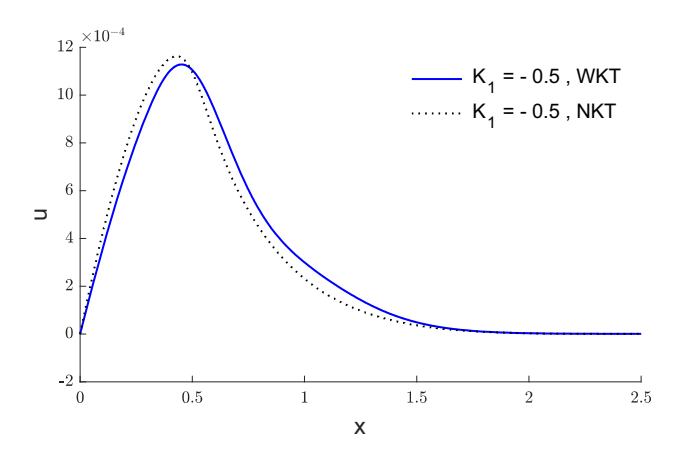


Figure 14: The displacement variation with and without the application of Kirchhoff's transform, considering the thermal conductivity parameter $k_1 = -0.5$.

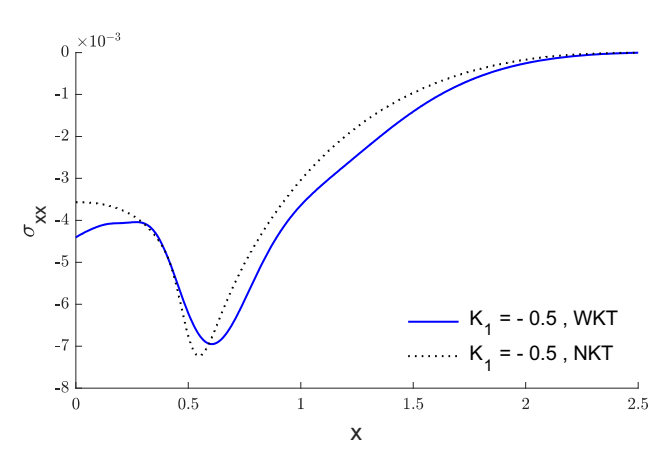


Figure 15: The stress variation with and without the application of Kirchhoff's transforms, considering the thermal conductivity parameter $k_1 = -0.5$.

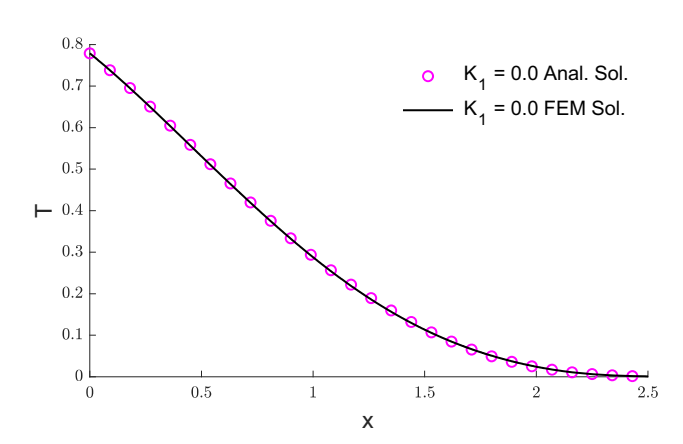


Figure 16: A comparison of changes in temperature when $k_1 = 0$: Results from analytical and FEM.

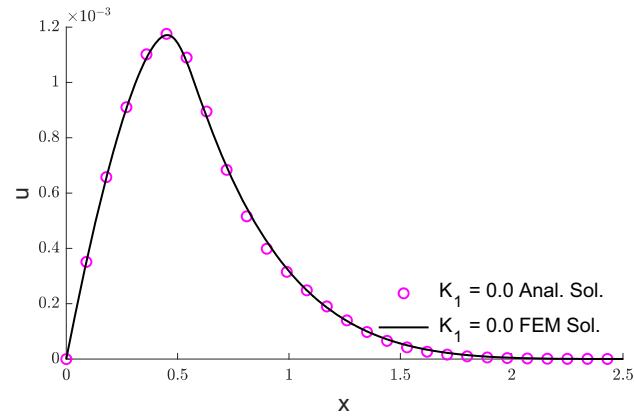


Figure 17: A comparison of changes in displacement when $k_1 = 0$: Results from analytical and FEM.

that the stress has a pattern, peaking at a negative number and then progressively declining to almost zero.

Figures 1–3 show a comparison of the outcomes obtained for physical parameters such as displacement, temperature, and stress, considering two models of thermoelasticity: the coupled theory without thermal relaxation time ($\tau_o = 0$) and the LS model with one relaxation time ($\tau_o = 0.05, 0.1, 0, ..., 15$) under varying thermal conductivity ($k_1 = -0.5$). As predicted, the relaxation time notably influences the distribution of the values of the studying variable.

The impacts of the exponent of the decayed heating flux ω on the distributions of all quantities along the distances are also investigated in Figures 4-6. As anticipated, the exponent of the decayed heating flux significantly affects the distributions of temperature, displacement, and stress values.

Without using the Kirchhoff transforms, Figures 7-9 show the effects of variable thermal conductivity on the studying variables via distance x (the nonlinear case). The distributions of the studying variables values are

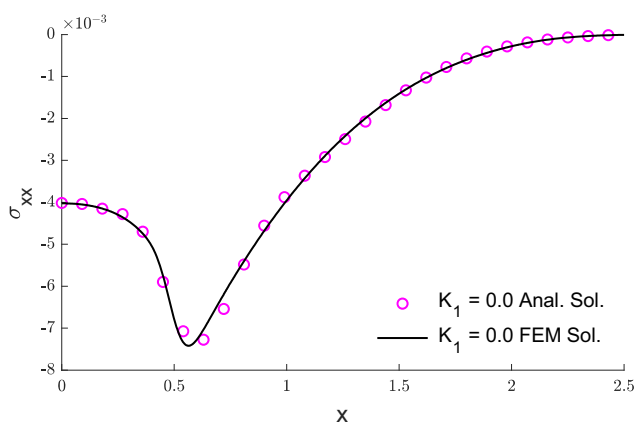


Figure 18: A comparison of changes in stress when $k_1 = 0$: Results from analytical and FEM.

significantly impacted by differences in thermal conductivity, as expected.

Figures 10–15 show a comparison of the results obtained when utilizing the Kirchhoff transform (WKT cases) *versus* not utilizing it (NKT cases). Specifically, these figures show the temperature variation, the displacement variation, and stress distribution *via* the distances x for k_1 values of –1.0 and –0.5. Notably, substantial differences can be seen between the WKT and NKT cases. When the Kirchhoff transform is employed (WKT), the variation of temperature, displacement, and stresses along x is smooth. However, when the Kirchhoff transform is not used (NKT), the variation is non-smooth and exhibits singular behaviors. This demonstrates the importance of incorporating the Kirchhoff transform for obtaining physically realistic solutions in this model.

Figures 16–18 show a comparison of the analytical solution obtained using the Laplace transform and the eigenvalue approaches with Kirchhoff transforms versus the numerical solution from the FEMs without using Kirchhoff transforms. This comparison is shown for the case where $k_{\rm I}=0$. The studying variable variations via the distances x, as obtained from the numerical solutions, show excellent agreement with the analytical results. This validates the finite-element implementation, demonstrating its ability to accurately solve this problem without requiring Kirchhoff transforms, even though the analytical solution was obtained using those transforms. The close match between numerical and analytical solutions confirms the robustness and reliability of the finite-element approach for this thermal stress analysis.

5 Conclusion

The transient thermoelastic response of materials under a time-decaying thermal field is examined in this work by employing nonlinear analysis techniques. The studying variable distributions were thoroughly understood by integrating varying thermal conductivity into a generalized thermoelasticity model with one thermal relaxation time. In solving nonlinear thermoelastic problems with variable thermal conductivity, the results demonstrate the robustness of the finite-element technique. This research study helps to comprehend the interactions existing between mechanical and thermal fields of a thermoelastic material which will further assist in better modeling in real applications.

Acknowledgments: This work was supported by the Princess Nourah bint Abdulrahman University Researchers Supporting Project number (PNURSP2025R518) and Princess Nourah bint Abdulrahman University, Riyadh, Saudi Arabia.

Funding information: This work was supported by the Princess Nourah bint Abdulrahman University Researchers Supporting Project number (PNURSP2025R518), and Princess Nourah bint Abdulrahman University, Riyadh, Saudi Arabia.

Author contributions: All authors have accepted responsibility for the entire content of this manuscript and consented to its submission to the journal, reviewed all the results and approved the final version of the manuscript. Conceptualization, Z.A., I.A., and A.A.; methodology, Z.A., I.A., and A.E.; software, Z.A., I.A., and A.E.; validation, I.A., A.E., and A.A.; formal analysis, I.A., A.E., and A.A.; investigation, Z.A., I.A., A.E., and A.A.; resources, A.A. All authors have read and agreed to publish version of the manuscript.

Conflict of interest: Authors state no conflict of interest.

References

- Noda N. Thermal stresses in materials with temperature-dependent properties. Appl Mech Rev. 1991;44(9):383–97.
- [2] Biot MA. Thermoelasticity and irreversible thermodynamics. J Appl Phys. 1956:27(3):240–53.
- [3] Lord HW, Shulman Y. A generalized dynamical theory of thermoelasticity. J Mech Phys Solids. 1967;15(5):299–309.
- [4] Green AE, Naghdi PM. Thermoelasticity without energy dissipation. J Elast. 1993;31(3):189–208.
- [5] Green A, Naghdi P. A re-examination of the basic postulates of thermomechanics. Proc R Soc Lond Ser A: Math Phys Sci. 1991;432(1885):171–94.
- [6] Hetnarski RB. Thermal stresses IV. North Holland: Elsevier; 1996.
- [7] Sherief H, Abd El-Latief AM. Effect of variable thermal conductivity on a half-space under the fractional order theory of thermoelasticity. Int | Mech Sci. 2013;74:185–9.
- [8] Mukhopadhyay S, Kumar R. Solution of a problem of generalized thermoelasticity of an annular cylinder with variable material properties by finite difference method. Comput Methods Sci Technol. 2009;15(2):169–76.
- [9] Sherief HH, Hamza FA. Modeling of variable thermal conductivity in a generalized thermoelastic infinitely long hollow cylinder. Meccanica. 2015;51(3):551–8.
- [10] Abbas I, Hobiny A, Marin M. Photo-thermal interactions in a semiconductor material with cylindrical cavities and variable thermal conductivity. J Taibah Univ Sci. 2020;14(1):1369–76.
- [11] Othman MIA, Abouelregal AE, Said SM. The effect of variable thermal conductivity on an infinite fiber-reinforced thick plate under initial stress. J Mech Mater Struct. 2019;14(2):277–93.
- [12] Ghasemi SE, Hatami M, Ganji DD. Thermal analysis of convective fin with temperature-dependent thermal conductivity and heat generation. Case Stud Therm Eng. 2014;4:1–8.
- [13] Xiong CB, Yu LN, Niu YB. Effect of variable thermal conductivity on the generalized thermoelasticity problems in a fiber-reinforced anisotropic half-space. Adv Mater Sci Eng. 2019;2019:1–9.
- [14] Khoukhi M, Abdelbaqi S, Hassan A. Transient temperature change within a wall embedded insulation with variable thermal conductivity. Case Stud Therm Eng. 2020;20:100645.

- [15] Abbas IA. Generalized magneto-thermoelasticity in a nonhomogeneous isotropic hollow cylinder using the finite element method. Arch Appl Mech. 2009;79(1):41-50.
- [16] Xiong CB, Guo Y. Effect of variable properties and moving heat source on magnetothermoelastic problem under fractional order thermoelasticity. Adv Mater Sci Eng. 2016;2016:1-12.
- [17] Zenkour AM, Abbas IA. A generalized thermoelasticity problem of an annular cylinder with temperature-dependent density and material properties. Int | Mech Sci. 2014;84:54-60.
- [18] Othman MI. Lord-Shulman theory under the dependence of the modulus of elasticity on the reference temperature in twodimensional generalized thermoelasticity. J Therm Stresses. 2002;25(11):1027-45.
- [19] Aboueregal AE, Sedighi HM. The effect of variable properties and rotation in a visco-thermoelastic orthotropic annular cylinder under the Moore-Gibson-Thompson heat conduction model. Proc Inst Mech Eng Part L-J Mater-Des Appl. 2021;235(5):1004-20.
- [20] Youssef HM, Abbas IA. Thermal shock problem of generalized thermoelasticity for an infinitely long annular cylinder with variable thermal conductivity. Comput Methods Sci Technol. 2007:13(2):95-100.
- [21] Singh S, Kumar D, Rai KN. Convective-radiative fin with temperature dependent thermal conductivity, heat transfer coefficient and wavelength dependent surface emissivity. Propuls Power Res. 2014;3(4):207-21.
- [22] Zhang H, Shang C, Tang G. Measurement and identification of temperature-dependent thermal conductivity for thermal insulation materials under large temperature difference. Int J Therm Sci. 2022;171:107261.
- [23] Pan W, Yi F, Zhu Y, Meng S. Identification of temperaturedependent thermal conductivity and experimental verification. Meas Sci Technol. 2016;27(7):075005.
- [24] Wang YZ, Zan C, Liu D, Zhou JZ. Generalized solution of the thermoelastic problem for the axisymmetric structure with temperature-dependent properties. Eur J Mech - A/Solids. 2019:76:346-54.
- [25] Wang YZ, Liu D, Wang Q, Zhou JZ. Thermoelastic interaction in functionally graded thick hollow cylinder with temperaturedependent properties. | Therm Stresses. 2018;41(4):399-417.
- [26] Wang Y, Liu D, Wang Q, Zhou J. Problem of axisymmetric plane strain of generalized thermoelastic materials with variable thermal properties. Eur J Mech - A/Solids. 2016;60:28-38.
- [27] Ezzat MA, El-Bary AA. On thermo-viscoelastic infinitely long hollow cylinder with variable thermal conductivity. Microsyst Technol. 2017;23(8):3263-70.
- [28] Hobiny A, Alzahrani F, Abbas I, Marin M. The effect of fractional time derivative of bioheat model in skin tissue induced to laser irradiation. Symmetry. 2020;12(4):1-10.
- [29] Abbas IA. A GN model for thermoelastic interaction in an unbounded fiber-reinforced anisotropic medium with a circular hole. Appl Math Lett. 2013;26(2):232-9.
- [30] Marin M, Florea O. On temporal behaviour of solutions in thermoelasticity of porous micropolar bodies. Analele Univ "Ovidius" Constanta - Ser Mat. 2014;22(1):169-88.
- [31] Bhatti MM, Marin M, Zeeshan A, Abdelsalam SI. Editorial: Recent trends in computational fluid dynamics. Front Phys. 2020;8:593111. doi: 10.3389/fphy.2020.593111.
- Alzahrani FS, Abbas IA. Analytical estimations of temperature in a living tissue generated by laser irradiation using experimental data. | Therm Biol. 2019;85:102421.

- [33] Hobiny A, Abbas I. Analytical solutions of fractional bioheat model in a spherical tissue. Mech Based Des Struct Mach. 2019;49(3):430-9.
- [34] Marin M, Seadawy A, Vlase S, Chirila A. On mixed problem in thermoelasticity of type III for Cosserat media. J Taibah Univ Sci. 2022;16(1):1264-74.
- Othman MI, Fekry M, Marin M. Plane waves in generalized magnetothermo-viscoelastic medium with voids under the effect of initial stress and laser pulse heating. Struct Eng Mech. 2020;73(6):621-9.
- [36] Marin M. Some estimates on vibrations in thermoelasticity of dipolar bodies. J Vib Control. 2010;16(1):33-47.
- [37] Cong PH, Duc ND. Nonlinear thermo-mechanical analysis of ES double curved shallow auxetic honeycomb sandwich shells with temperature-dependent properties. Compos Struct. 2022;279:114739.
- [38] Shahmohammadi MA, Mirfatah SM, Emadi S, Salehipour H, Civalek Ö, Nonlinear thermo-mechanical static analysis of toroidal shells made of nanocomposite/fiber reinforced composite plies surrounded by elastic medium. Thin-Walled Struct. 2022;170:108616.
- [39] Tornabene F, Viscoti M, Dimitri R. Thermo-mechanical analysis of laminated doubly-curved shells: Higher order equivalent layer-wise formulation. Compos Struct. 2024;335:117995.
- [40] Farokhi H, Ghayesh MH. Nonlinear thermo-mechanical behaviour of MEMS resonators. Microsyst Technol. 2017;23:5303-15.
- Youssef H. State-space approach on generalized thermoelasticity [41] for an infinite material with a spherical cavity and variable thermal conductivity subjected to ramp-type heating. Can Appl Math Quaterly. 2005;13:4.
- [42] Zenkour AM, Abbas IA. Nonlinear transient thermal stress analysis of temperature-dependent hollow cylinders using a finite element model. Int J Struct Stab Dyn. 2014;14(7):1450025.
- [43] Abbas IA, Kumar R. 2D deformation in initially stressed thermoelastic half-space with voids. Steel Compos Struct. 2016;20(5):1103-17.
- [44] Abbas IA. Eigenvalue approach on fractional order theory of thermoelastic diffusion problem for an infinite elastic medium with a spherical cavity. Appl Math Model. 2015;39(20):6196-206.
- [45] Abbas IA, Abdalla AENN, Alzahrani FS, Spagnuolo M. Wave propagation in a generalized thermoelastic plate using eigenvalue approach. J Therm Stresses. 2016;39(11):1367-77.
- Othman MIA, Abbas IA. Eigenvalue approach for generalized thermoelastic porous medium under the effect of thermal loading due to a laser pulse in DPL model. Indian J Phys. 2019;93(12):1567-78.
- [47] Kumar R, Miglani A, Rani R. Eigenvalue formulation to micropolar porous thermoelastic circular plate using dual phase lag model. Multidiscipline Modeling in. Mater Struct. 2017;13(2):347-62.
- Kumar R, Miglani A, Rani R. Analysis of micropolar porous thermoelastic circular plate by eigenvalue approach. Arch Mech. 2016;68(6):423-39.
- [49] Gupta ND, Das NC. Eigenvalue approach to fractional order generalized thermoelasticity with line heat source in an infinite medium. J Therm Stresses. 2016;39(8):977-90.
- Santra S, Lahiri A, Das NC. Eigenvalue approach on thermoelastic interactions in an infinite elastic solid with voids. J Therm Stresses. 2014;37(4):440-54.
- Baksi A, Roy BK, Bera RK. Eigenvalue approach to study the effect of [51] rotation and relaxation time in generalized magneto-thermoviscoelastic medium in one dimension. Math Comput Model. 2006;44(11-12):1069-79.
- [52] Das NC, Lahiri A, Giri RR. Eigenvalue approach to generalized thermoelasticity. Indian | Pure Appl Math. 1997;28(12):1573-94.
- [53] Stehfest H. Algorithm 368: Numerical inversion of Laplace transforms [D5]. Commun ACM. 1970;13(1):47-9.